

# High-temperature poling treatment of congruent ferroelectric $\text{LiNb}_{0.5}\text{Ta}_{0.5}\text{O}_3$ solid solution single crystals

Anatolii A. Mololkin<sup>1,2</sup>, Dmitry V. Roshchupkin<sup>2</sup>, Eugenii V. Emelin<sup>2</sup>, Rashid R. Fahrtdinov<sup>2</sup>

<sup>1</sup> JSC Fomos-Materials, 16 Buzheninova Str., Moscow 107023, Russia

<sup>2</sup> Institute of Microelectronics Technology and High-Purity Materials of the Russian Academy of Sciences, 6 Academician Ossipyan Str., Chernogolovka, Moscow Region 142432, Russia

Corresponding author: Anatolii A. Mololkin (Anatoli.mololkin.sooth@mail.ru)

Received 23 February 2021 ♦ Accepted 2 March 2021 ♦ Published 30 March 2021

**Citation:** Mololkin AA, Roshchupkin DV, Emelin EV, Fahrtdinov RR (2021) High-temperature poling treatment of congruent ferroelectric  $\text{LiNb}_{0.5}\text{Ta}_{0.5}\text{O}_3$  solid solution single crystals. *Modern Electronic Materials* 7(1): 17–20. <https://doi.org/10.3897/j.moem.7.1.66773>

## Abstract

Lithium niobate and tantalate are among the most important and widely used materials of acoustooptics and acoustoelectronics. They have high piezoelectric constants enabling their use as actuators. Their use is however restricted by the thermal instability of lithium niobate crystals and the low Curie temperature  $T_C$  of lithium tantalate crystals. Overcoming these drawbacks typical of some compounds is possible by growing  $\text{LiNb}_{1-x}\text{Ta}_x\text{O}_3$  single crystals. Good quality  $\text{LiNb}_{1-x}\text{Ta}_x\text{O}_3$  single crystals have been grown using the Czochralsky technique. High-temperature poling process of  $\text{LiNb}_{1-x}\text{Ta}_x\text{O}_3$  single crystals has been studied. The main differences between the process modes required for poling of congruent  $\text{LiNb}_{1-x}\text{Ta}_x\text{O}_3$  single crystals and congruent  $\text{LiNbO}_3$  single crystals have been demonstrated. Parameters of high-temperature electric diffusion processing of  $\text{LiNb}_{1-x}\text{Ta}_x\text{O}_3$  single crystals that provide for singledomain crystals for further study of physical properties have been reported.

## Keywords

lithium niobate, lithium tantalate, ferroelectric crystals, high-temperature single domain poling process, crystal growth, actuators.

## 1. Introduction

The development of acoustooptic devices for real time transmission and processing of acoustic signals is mainly fueled by the search for new materials having good acoustic properties [1–3]. From this viewpoint of great interest are ferroelectric crystals of  $\text{LiNbO}_3$  and  $\text{LiTaO}_3$ . These materials have high piezoelectric constants enabling their

use as actuators [4–6]. Their use is however restricted by the thermal instability of lithium niobate crystals and the low Curie temperature  $T_C$  of lithium tantalate crystals. Growing  $\text{LiNb}_{1-x}\text{Ta}_x\text{O}_3$  single crystals will help eliminating these drawbacks typical of some compounds.

Growth of  $\text{LiNb}_{1-x}\text{Ta}_x\text{O}_3$  solid solution single crystals was dealt with earlier [7–9]. However obtaining good quality  $\text{LiNb}_{1-x}\text{Ta}_x\text{O}_3$  single crystals for further study of physical properties failed. All attempts to

grow  $\text{LiNb}_{1-x}\text{Ta}_x\text{O}_3$  single crystals yielded crystals with a large number of defects, e.g. cracks, twins, gas inclusions and pores.

Results for Czochralsky growth of  $\text{LiNb}_{1-x}\text{Ta}_x\text{O}_3$  single crystals were reported [10] and the size and quality of the crystals enabled a study of their structure and physical properties. Ferroelectric  $\text{LiNb}_{1-x}\text{Ta}_x\text{O}_3$  single crystals were grown by the Czochralsky method. However during their growth a poly-domain crystal formed which is energetically favorable for ferroelectric crystals. For the formation of a single-domain crystal the as-synthesized poly-domain crystal is heated to the Curie temperature and an electric field is applied along the polar Z axis of the crystal thus achieving the single-domain state. It is worth mentioning that the Curie temperatures differ between compounds of the  $\text{LiNbO}_3$ – $\text{LiTaO}_3$  system [10].  $T_C$  for stoichiometric  $\text{LiNbO}_3$  crystals is 1190 °C while for stoichiometric  $\text{LiTaO}_3$  crystals it is 660 °C. These differences in  $T_C$  should be taken into account during the poling process, in order to obtain single-domain  $\text{LiNb}_{1-x}\text{Ta}_x\text{O}_3$  crystals.

Thus studying the properties and technological modes of thermoelectric processing for achieving the defect-free unipolar state of  $\text{LiNb}_{1-x}\text{Ta}_x\text{O}_3$  crystals for different ratios of the isomorphous cations Nb/Ta is an important task. The most interesting and complex task is poling of solid solution crystals with a 1 : 1 ratio of the isomorphous cations into a single-domain state because their high-temperature poling process parameters will differ strongly from those of the edge-composition  $\text{LiNbO}_3$  and  $\text{LiTaO}_3$  compounds.

## 2. Growth of $\text{LiNb}_{1-x}\text{Ta}_x\text{O}_3$ crystals

$\text{LiNb}_{0.5}\text{Ta}_{0.5}\text{O}_3$  crystals were grown using the Czochralsky technique in a modified induction heated NIKA-3M plant with automatic crystal diameter control. The crystals were grown in a 60 mm diam. and 60 mm high platinum crucible by pulling along the polar Z axis. The Curie temperature of the  $\text{LiNb}_{0.5}\text{Ta}_{0.5}\text{O}_3$  crystals, at which the paraelectric phase transits into the ferroelectric phase, ranges from 607 to 1190 °C and depends primarily on the Nb/Ta cation ratio.

Small good quality  $\text{LiNb}_{0.5}\text{Ta}_{0.5}\text{O}_3$  crystals were grown. Figure 1 shows the appearance of an as-grown  $\text{LiNb}_{0.5}\text{Ta}_{0.5}\text{O}_3$  crystal. The diameter of the cylindrical part of the crystal varied in the 12–14 mm range, the length of the cylindrical part was 14 mm.

## 3. High-temperature poling treatment of $\text{LiNb}_{1-x}\text{Ta}_x\text{O}_3$ crystals

The as-grown  $\text{LiNb}_{1-x}\text{Ta}_x\text{O}_3$  crystals are poly-domain ones because this condition provides for the minimum energy of the polar crystals. However, single crystals with a perfect crystalline structure are used in acoustoelectro-

tics. One should therefore carry out the poling process of the as-grown crystals which is the key post-growth operation. The aim of this operation is to achieve a unipolar state of the crystal and eliminate micro- and macrodefects in the structure of the ferroelectric  $\text{LiNb}_{1-x}\text{Ta}_x\text{O}_3$  crystals by implementing electric diffusion processes.

The process modes and properties of high-temperature poling treatment of congruent undoped  $\text{LiNbO}_3$  and  $\text{LiTaO}_3$  single crystals were described earlier, e.g. [11–13]. Poling process in congruent doped  $\text{LiNbO}_3$  single crystals were also studied in detail [14, 15]. Since pore- and crack-free  $\text{LiNb}_{1-x}\text{Ta}_x\text{O}_3$  single crystals cannot be grown there are no literary data on the process modes of high-temperature poling procedure for these crystals. Before poling the crystal was butt-machined and ground at the bottom and top surfaces in order for the crystal surface to have no deviation from planarity. High-temperature electric diffusion processing was conducted in a software controlled furnace. An Alundum ceramic pad with a plate-shaped platinum electrode was placed into the furnace chamber. A ground plane-parallel  $\text{LiNbO}_3$  plate was placed onto the electrode in order to avoid electrode soldering to the crystal and provide for the best possible contact between the electrode and the crystal. Then the test  $\text{LiNb}_{0.5}\text{Ta}_{0.5}\text{O}_3$  crystal was placed onto the plate and one more plane-parallel  $\text{LiNbO}_3$  plate was placed onto the test crystal. Finally a plate-shaped platinum electrode was placed onto the plate and the electrodes were connected to a power source.

Figure 2 (Curve 1) shows schematic of congruent  $\text{LiNb}_{0.5}\text{Ta}_{0.5}\text{O}_3$  crystal poling process mode in an electric field taking into account the crystal dimensions and  $T_C \approx 900$  °C. The standard mode for congruent  $\text{LiNbO}_3$  crystals was used, which consisted of several stages:

- heating to ~1000 °C and exposure for ~30 min at ~1000 °C;
- connection of bias and specimen exposure for ~30 min;
- cooling under bias at a 100 K/h rate to ~800 °C;
- bias disconnection and further cooling to room temperature at the same cooling rate.

The positive electrode of the power source was connected to the bottom part of the crystal, i.e., the one clos-



Figure 1.  $\text{LiNb}_{0.5}\text{Ta}_{0.5}\text{O}_3$  crystal grown along the polar Z axis.

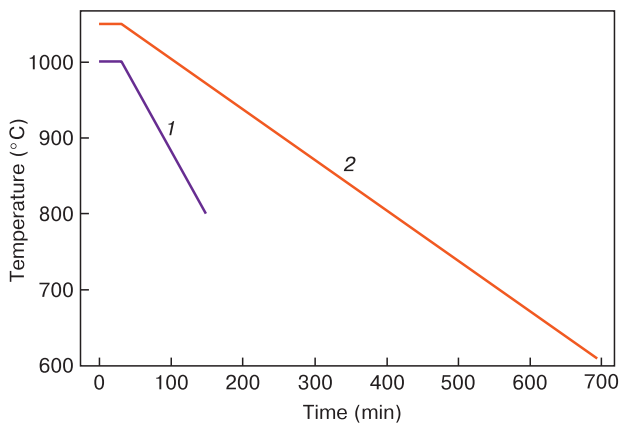


**Figure 2.** Congruent  $\text{LiNb}_{0.5}\text{Ta}_{0.5}\text{O}_3$  crystal poling process mode: (1) conventional mode used for congruent lithium niobate crystals taking into account crystal dimensions and  $T_C \approx 900^\circ\text{C}$ ; (2) poling process mode adapted to  $\text{LiNb}_{0.5}\text{Ta}_{0.5}\text{O}_3$ .

er to the end of the as-grown crystal, and the negative electrode was connected to the crystal's top part which is closer to the seed. The poling current was chosen so the current density on the contact surface is within  $2\text{ mA/cm}^2$ . The process was conducted in current stabilization mode, the poling current being  $1\text{ mA}$ .

Studies of the macro- and microdefect structure of the crystals were conducted with an optical method using Hi-rox KH-8700 laboratory microscope. The specimens after high-temperature thermoelectric processing were ground, polished and chemically etched at room temperature for 2 h in hydrofluoric acid (HF). Figure 3 a shows the microstructure of the top portion of the single crystal specimen which contained discrete multifaceted micro-domains with opposite signs, indicating a high degree of unipolarity of the domain structure. Figure 3 b shows the microstructure of the bottom portion of the single crystal specimen which remained a poly-domain one indicating that much more energy and time should be spent for the complete poling of the  $\text{LiNb}_{0.5}\text{Ta}_{0.5}\text{O}_3$  crystal.

Figure 2 b shows schematic of the poling process adapted to  $\text{LiNb}_{0.5}\text{Ta}_{0.5}\text{O}_3$  crystals. The main differences from the conventional process were as follows:

- the duration of exposure under bias was chosen taking into account crystal dimensions (for specimens up to  $20\text{ mm}$  in diameter and up to  $30\text{ mm}$  in length the bias exposure duration was  $30\text{ min}$ );
- the exposure temperature for  $\text{LiNb}_{0.5}\text{Ta}_{0.5}\text{O}_3$  solid solution crystals was chosen based on the  $\text{LiNbO}_3\text{--LiTaO}_3$  system phase diagram [7] (for more effective solid state electrolysis one should increase the exposure temperature to  $T_C + 150^\circ\text{C}$ );
- poling currents were chosen empirically so the current density on the contact surface is within  $2\text{ mA/cm}^2$ . For a Nb/Ta cation ratio of 1, the initial electric field magnitude on the crystal surface should be at least  $10\text{ V}\cdot\text{cm}^{-1}$  (the poling current is  $\sim 2\text{ mA}$ ). Lower currents do not provide for the complete poling of the  $\text{LiNb}_{0.5}\text{Ta}_{0.5}\text{O}_3$  crystals. Connection to bias at sufficiently high temperatures

leads to solid state electrolysis of the crystal which favors the redistribution of intrinsic and extrinsic elements across the crystal;

- the cooling rate of the crystal under bias should be within  $40\text{ K/h}$  for small crystals and within  $25\text{ K/h}$  for larger crystals;
- the temperature at which bias is disconnected should be such that the current passing through the crystal at this voltage is close to zero. Otherwise this will initiate inverse repolarization with the formation of micro-domains as illustrated in Fig. 3 b.

Figure 4 a shows the microstructure of the top part of the  $\text{LiNb}_{0.5}\text{Ta}_{0.5}\text{O}_3$  single crystal specimen after adapted poling process. By analogy with the conventional poling process the microstructure contained a small quantity of discrete domains with opposite signs which could not be repolarized. Most likely these domains attached to the defect structure of the crystal. Figure 4 b shows the microstructure of the bottom part of the  $\text{LiNb}_{0.5}\text{Ta}_{0.5}\text{O}_3$  single crystal specimen after adapted poling process. One can see a more homogeneous domain structure in comparison with that after the conventional process. The microstructure contains discrete multifaceted micro-domains sized up to  $30\text{ }\mu\text{m}$ . Furthermore one can see microdefects in the form of dark spots and strips sized above  $100\text{ }\mu\text{m}$  for which the chemical etching rate differs from that for the crystal matrix. This fact indicates that the bottom part of the single crystal specimen

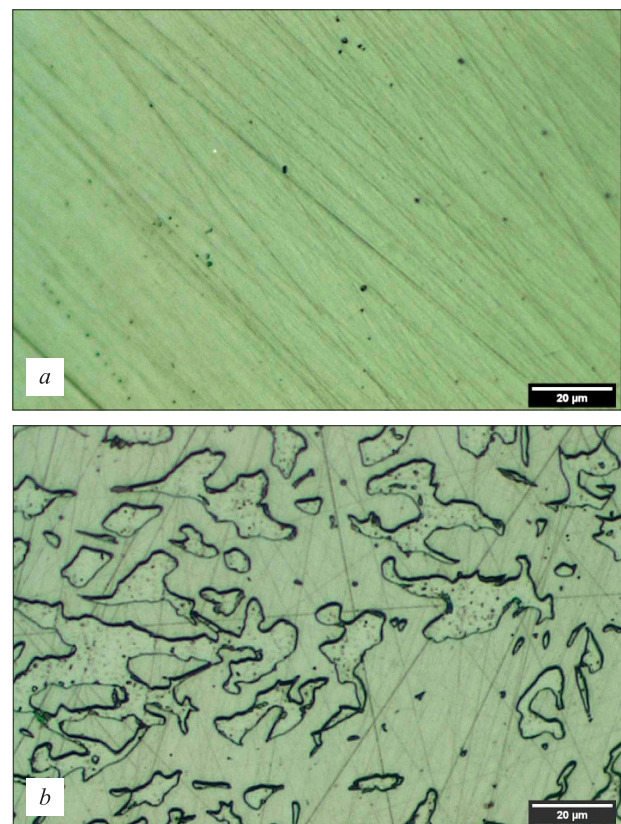


**Figure 3.** Microstructure of  $\text{LiNb}_{0.5}\text{Ta}_{0.5}\text{O}_3$  crystal after conventional poling process: (a and b) top and bottom portions of single crystal specimen.

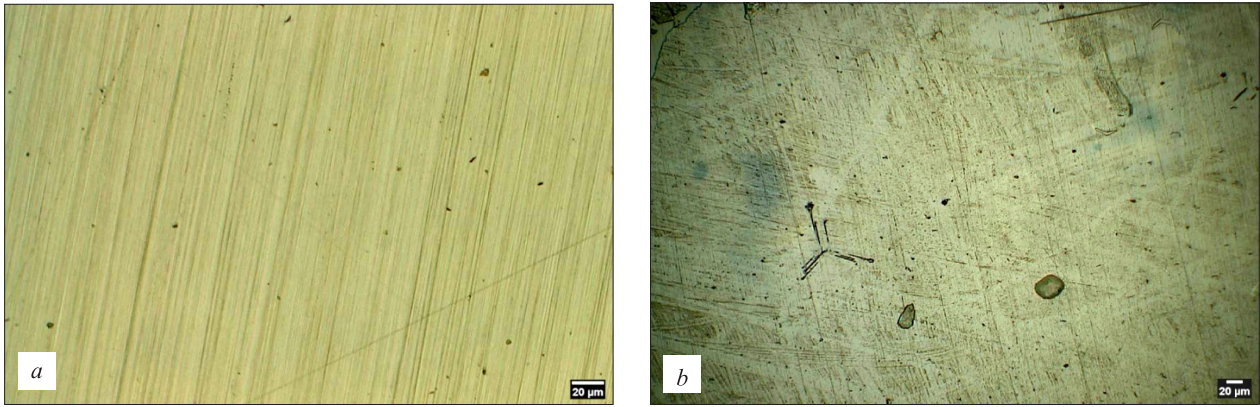


**Figure 4.** Microstructure of  $\text{LiNb}_{0.5}\text{Ta}_{0.5}\text{O}_3$  crystal after adapted poling process: (a and b) top and bottom portions of single crystal specimen.

contains phases with a variable composition differing from that of the  $\text{LiNb}_{0.5}\text{Ta}_{0.5}\text{O}_3$  phase.

## 4. Conclusion

Small good quality ferroelectric crystals of the complex composition  $\text{LiNb}_{0.5}\text{Ta}_{0.5}\text{O}_3$  were grown. The properties

of high-temperature poling process of  $\text{LiNb}_{0.5}\text{Ta}_{0.5}\text{O}_3$  single crystals were studied. The main differences between the process modes required for poling of congruent  $\text{LiNb}_{1-x}\text{Ta}_x\text{O}_3$  single crystals and congruent  $\text{LiNbO}_3$  single crystals were demonstrated. Parameters of high-temperature electric diffusion processing of  $\text{LiNb}_{1-x}\text{Ta}_x\text{O}_3$  single crystals that provide for single-domain single crystals for further study of physical properties were reported.

## References

1. Kaino G. *Akusticheskie volny* [Acoustic waves]. Moscow: Mir, 1990. 652 p. (In Russ.)
2. Yariv A., Yuh P. *Opticheskie volny v kristallah* [Optical waves in crystals]. Moscow: Mir, 1987. 616 p. (In Russ.)
3. Campbell C. Surface acoustic wave devices and their signal processing applications. Academic Press, 1989. 470 p. <https://doi.org/10.1016/B978-0-12-157345-4.X5001-2>
4. Nakamura K., Nakamura T., Yamada K. Torsional actuators using  $\text{LiNbO}_3$  plates with an inversion layer. *Jpn. J. Appl. Phys.* 1993; 32(5B): 2415–2417. <https://doi.org/10.1143/JJAP.32.2415>
5. Nakamura K., Shimizu H. Hysteresis-free piezoelectric actuators using  $\text{LiNbO}_3$  plates with a ferroelectric inversion layer. *Ferroelectrics*. 1989; 93(1): 211–216. <https://doi.org/10.1080/00150198908017348>
6. Ueda M., Sawada H., Tanaka A., Wakatsuki N. Piezoelectric actuator using a  $\text{LiNbO}_3$  bimorph for an optical switch. *IEEE Symposium on Ultrasonics*. 1990: 1183–1186. <https://doi.org/10.1109/ULTSYM.1990.171548>
7. Fukuda T., Hirano H. Solid-solution  $\text{LiTa}_x\text{Nb}_{1-x}\text{O}_3$  single crystal growth by Czochralski and edge-defined film-fed growth technique. *J. Crystal Growth*. 1976; 35(2): 127–132. [https://doi.org/10.1016/0022-0248\(76\)90159-7](https://doi.org/10.1016/0022-0248(76)90159-7)
8. Shimura F., Fujino Y. Crystal growth and fundamental properties of  $\text{LiNb}_{1-y}\text{Ta}_y\text{O}_3$ . *J. Crystal Growth*. 1977; 38(3): 293–302. [https://doi.org/10.1016/0022-0248\(77\)90349-9](https://doi.org/10.1016/0022-0248(77)90349-9)
9. Bartasyte A., Glazer A.M., Wondre F., Prabhakaran D., Thomas P.A., Huband S., Keeble D.S., Margueron S. Growth of  $\text{LiNb}_{1-x}\text{Ta}_x\text{O}_3$  solid solution crystals. *Materials Chemistry and Physics*. 2012; 134: 728–735. <https://doi.org/10.1016/j.matchemphys.2012.03.060>
10. Roshchupkin D., Emelin E., Plotitsyna O., Fahrtdinov R., Irzhak D., Karandashev V., Orlova T., Targonskaya N., Sakharov S., Mololkin A., Redkin B., Fritze H., Suhak Y., Kovalev D., Vadilonga S., Ortega L., Leitenberger W. Single crystals of ferroelectric lithium niobate-tantalate  $\text{LiNb}_{(1-x)}\text{Ta}_x\text{O}_3$  solid solutions for high-temperature sensor and actuator applications. *Acta Cryst.* 2020; B76: 1071–1076. <https://doi.org/10.1107/S2052520620014390>
11. Kuz'minov Yu.S. *Niobat i tantalat litiya: materialy dlya nelineinoi optiki* [Lithium niobate and tantalate: materials for nonlinear optics]. Moscow: Nauka, 1975. 52 p. (In Russ.)
12. Kuz'minov Yu.S. *Elektroopticheskiy i nelineynoy opticheskiy kristall niobata litiya* [Electro-optical and nonlinear optical crystal of lithium niobate]. Moscow: Nauka, 1987. 262 p. (In Russ.)
13. Blistanov A.A. *Krystally kvantovoy i nelineynoy optiki* [Crystals of quantum and nonlinear optics]. Moscow: MISiS, 2000. 197 p. (In Russ.)
14. Grabmaier B.C., Otto F. Growth and investigation of MgO-doped  $\text{LiNbO}_3$ . *J. Crystal Growth*. 1986; 79(1–3): 682–688. [https://doi.org/10.1016/0022-0248\(86\)90537-3](https://doi.org/10.1016/0022-0248(86)90537-3)
15. Palatnikov M.N., Sidorov N.V., Makarova O.V., Birjukova I.V. Features of the postgrowth thermal and electrothermal treatment of nominally pure and heavily doped lithium-niobate crystals. *Bulletin of the Russian Academy of Sciences: Physics*. 2018; 82(3): 314–316. <https://doi.org/10.3103/S1062873818030176>